JOURNAL OF AGRICULTURAL AND FOOD CHEMISTRY

Article

pubs.acs.org/JAFC

Density Functional Predictions of Antioxidant Activity and UV Spectral Features of Nasutin A, Isonasutin, Ellagic Acid, and One of Its Possible Derivatives

Gloria Mazzone,*[,†] Marirosa Toscano,[†] and Nino Russo[†,§]

[†]Dipartimento di Chimica e Tecnologie Chimiche, Università della Calabria, I-87036 Arcavacata di Rende, Italy

[§]Departamento de Quimica, Division de Ciencias Basicas e Ingenieria, Universidad, Autonoma Metropolitana-Iztapalapa, Av. San Rafael Atlixco No. 186, Col. Vicentina, CP 09340, Mexico, D.F., Mexico

Supporting Information

ABSTRACT: The antioxidant ability of ellagic acid and some of its derivatives was explored at density functional level of theory within the framework of the following three different reaction mechanisms: hydrogen atom transfer (HAT), electron transfer followed by proton transfer (SET-PT), and sequential proton loss electron transfer (SPLET). Computations were performed in gas phase and in both water and methanol media. Results show that the HAT mechanism is preferred by this class of compounds in all environments, although, in principle, polar solvents should promote the SET-PT and SPLET mechanisms. Among the considered compounds, the derivative not yet experimentally characterized seems to be the most promising candidate as antioxidant. For a more detailed spectroscopic characterization and to help in the identification of these compounds, the simulated UV spectra of all investigated molecules were done by using the time-dependent formulation of density functional theory (TDDFT).

KEYWORDS: *ellagic acid, nasutin A, isonasutin, DFT, antioxidant properties, UV spectra*

INTRODUCTION

Ellagic acid is a polyphenol dimeric derivative of gallic acid. It is the product of acidic hydrolysis of ellagitannins via hexahydroxydiphenic acid formation, which spontaneously lactonizes to ellagic acid. The ellagitannins are present in a wide variety of fruits, berries, and oak-aged wines, including raspberries, strawberries, blackberries, cranberries, pomegranate, and some nuts such as pecans and walnuts,[1−9] but the highest levels of ellagic acid are found in raspberries. The hydrolysis of ellagitannins and the following removal of the ellagic acid hydroxyls in the 3- and 3′-positions or in the 4- and 3′-positions, without opening of the lactone rings, produces nasutin A and isonasutin derivatives, respectively. They were first found in some Australian termites about 40 years ago.[10,11] Recently, it was hypothesized that also other ellagic acid derivatives, differing by the −OH group ring positions, can be produced as intermediates during ellagitannin metabolism.[12]

Similarly to many other polyphenols, ellagitannins, ellagic acid, and their derivatives possess a wide range of biological activities, such as antioxidant, anticarcinogenic, antifibrosis, antiplasmodial, anti-inflammatory, antimicrobial, prebiotic, and chemopreventive activities, which suggest they could have strong beneficial effects on human health.[13−24] These effects are principally related to the prevention of cardiovascular diseases and cancer and can be ascribed to the potent free radical scavenging activity that these compounds exert in vitro.

In recent years, much interest has been devoted to the study of phenol-based compounds, and many methods, both experimental and theoretical, have been developed to quantify their antioxidant capabilities in biological materials.[25−27]

Antioxidants can delay, inhibit, or prevent the oxidation of compounds, trapping free radicals and reducing oxidative stress, reacting with them at a rate faster than the substrate.

The main mechanisms by which an antioxidant (ArOH) can deactivate a free radical are as follows:

hydrogen atom transfer (HAT)

$$\mathrm{ArOH + ROO^{\bullet} \rightarrow ArO^{\bullet} + ROOH} \quad (1)$$

single-electron transfer followed by proton transfer (SET-PT)

$$\mathrm{ArOH + ROO^{\bullet} \rightarrow ArOH^{+\bullet} + ROO^{-}} \quad (2.1)$$

$$\mathrm{ArOH^{\bullet +} \rightarrow ArO^{\bullet} + H^{+}} \quad (2.2)$$

$$\mathrm{ROO^{-} + H^{+} \rightarrow ROOH} \quad (2.3)$$

sequential proton loss electron transfer (SPLET)

$$\mathrm{ArOH \rightarrow ArO^{-} + H^{+}} \quad (3.1)$$

$$\mathrm{ArO^{-} + ROO^{\bullet} \rightarrow ArO^{\bullet} + ROO^{-}} \quad (3.2)$$

$$\mathrm{ROO^{-} + H^{+} \rightarrow ROOH} \quad (3.3)$$

Although the final result for SET-PT and SPLET is the same as in the HAT mechanism, the rate-limiting step is different. In the HAT mechanism (reaction 1), the free radical removes a hydrogen atom from the antioxidant that becomes itself a radical. Therefore, the bond dissociation enthalpy (BDE) of the

Received: July 25, 2013
Revised: September 11, 2013
Accepted: September 11, 2013
Published: September 11, 2013

O−H bonds is an important parameter in evaluating the antioxidant action. A lower BDE results in an easier O−H bond breaking. In the SET-PT (reactions 2), the radical cation is first formed and afterward deprotonated. The adiabatic ionization potential and O−H proton dissociation enthalpy (PDE) describe the energetics of this process. Low IP values increase the possibility of forming a superoxide anion radical enhancing the antioxidant activity. In the SPLET mechanism (reactions 3), the reaction enthalpy of the first step corresponds to the proton affinity (PA) of the phenoxide anion (ArO^-), whereas the electron transfer enthalpy (ETE) should be taken into account for the second step, in which an electron transfer from phenoxide anion to $ROO^\bullet$ radical occurs.

Within the framework of molecular orbital theory, important information on the working mechanism of antioxidant can come from the knowledge of the frontier orbital energies, E_{HOMO} and E_{LUMO}. The lower is the HOMO energy, the weaker is the molecule donating electron ability. On the contrary, a higher HOMO energy implies that the molecule is a good electron donor, whereas E_{LUMO} represents the ability of a molecule receiving electron.[28] Because the H abstraction reaction involves electron transfer, the HOMO composition of a phenolic compound can give a qualitative idea of its active site for scavenging free radical activity.

We report here a density functional study on the antioxidant activity of isonasutin (**2**), nasutin A (**3**), ellagic acid (**1**), and one of its recently predicted derivatives (**4**) (Scheme 1) that is not yet identified in nature.[12] To help in the identification of this latter compound, UV spectra were simulated for all of the investigated systems. In this way we will be able to assess the reliability of our results through the comparison of existing data and propose for the first time the spectrum of the compound not yet identified.

Scheme 1

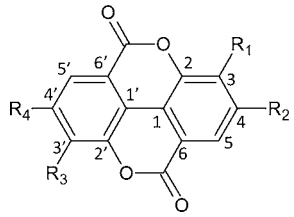

1. R_1=R_2=R_3=R_4=OH
2. R_1=R_4=OH; R_2=R_3=H
3. R_2=R_4=OH; R_1=R_3=H
4. R_1=R_2=R_4=OH; R_3=H

COMPUTATIONAL DETAILS

All calculations have been performed using the Gaussian 03 computational package.[29] The geometries of all the phenolic compounds investigated, including radicals, radical cations, and anions, have been fully optimized in the gas phase and both water and methanol media at the DF level employing the hybrid exchange functional by Becke (B3) in combination with the Lee, Yang, and Parr (LYP) correlation functional.[30,31] For all of the optimization calculations the basis set 6-31+G** was used for all of the atoms. The solvation effects were computed by using the conductor polarizable continuum model (CPCM)[32] as implemented in Gaussian 03. The UAHF set of radii has been used to build up the cavity. To simulate both water and methanol solvents the dielectric constant values of 78.3553 and 32.613 were used, respectively.

All of the optimized structures were confirmed to be real minima by harmonic vibrational frequencies calculations.

The unrestricted open-shell approach was used for radical species. No spin contamination was found for any of the radicals, the $\langle S^2 \rangle$ value being about 0.750 in all cases.

Final energies were calculated by performing single-point calculations on the optimized geometries at the same level of theory and employing the large 6-311++G(3df,2p) standard basis sets for all of the atoms.

Computations of single-point spin densities were performed using the above-mentioned protocol for the most stable radicals of all the investigated compounds.

This computational protocol was already successfully used in the determination of antioxidant properties for a large series of polyphenols.[33−39]

BDE, IP, PDE, PA, and ETE were determined in gas phase and in both water and methanol solvents at 298 K by using the following expressions:

$$BDE = H(ArO^\bullet) + H(H^\bullet) - H(ArOH)$$

$$IP = H(ArOH^{\bullet+}) + H(H^+) - H(ArOH)$$

$$PDE = H(ArO^\bullet) + H(H^+) - H(ArOH^{\bullet+})$$

$$PA = H(ArO^-) + H(H^+) - H(ArOH)$$

$$ETE = H(ArO^\bullet) + H(e^-) - H(ArO^-)$$

The $H(H^+)$ and $H(e^-)$ enthalpy values were taken from experiment.[40] However, theoretical determination of these quantities is available in a previous DF study on some phenolic derivatives.[41] Absorption spectra were computed as vertical electronic excitations from the minima of the ground-state structures by using time-dependent density functional response theory[42] as implemented in the Gaussian 03 code. These calculations were carried out by using the standard 6-31+G** basis sets and the same B3LYP exchange-correlation functional in methanol medium.

RESULTS AND DISCUSSION

Molecular Geometry and Radical Stability. The optimized structures of compounds are reported in Figure S1 of the Supporting Information, whereas selected geometric parameters and relative enthalpies of their radicals are reported in Tables 1 and 2, respectively.

Table 1. Selected Geometric Parameters of Compounds 1−4 Calculated in Gas Phase at the B3LYP Level (Available Experimental Data in Parentheses)

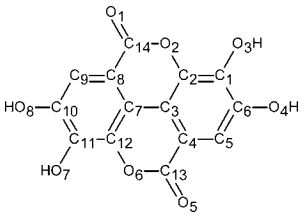

	1	2	3	4
C1−C2 (Å)	1.395 (1.386)[a]	1.402	1.388	1.394
C1−C6 (Å)	1.416 (1.411)	1.407	1.406	1.417
C1−O3 (Å)	1.351 (1.351)	1.353		1.351
C6−O4 (Å)	1.366 (1.347)		1.362	1.366
C3−C7 (Å)	1.427 (1.430)	1.427	1.423	1.425
C2−O2 (Å)	1.375 (1.383)	1.378	1.378	1.377
O2−C14 (Å)	1.387 (1.379)	1.380	1.385	1.383
C14−O1 (Å)	1.217 (1.209)	1.215	1.215	1.215
O2−C14−C8 (deg)	117.5 (118.7)	117.4	117.5	117.5
C1−C6−O4 (deg)	113.7 (113.7)		121.8	113.5

[a]Reference 32.

As far as ellagic acid (**1**) molecular geometry is concerned, we can emphasize the good agreement between theoretical and

dx.doi.org/10.1021/jf403262k | J. Agric. Food Chem. 2013, 61, 9650−9657

Table 2. B3LYP/6-311++G(3df,2p) Relative Enthalpy Energies (ΔE in kcal/mol) Calculated for All Radicals Investigated in Gas Phase and in Both Methanol and Water Environments

compd	ΔE (kcal/mol) vacuum	methanol	water
1			
radical 3OH	7.6	4.4	4.3
radical 4OH	0.0	0.0	0.0
2			
radical 3OH	0.6	0.2	0.2
radical 4′OH	0.0	0.0	0.0
3			
radical 4OH	0.0	0.0	0.0
4			
radical 3OH	8.3	5.0	4.5
radical 4OH	0.0	0.0	0.0
radical 4′OH	7.8	6.0	5.9

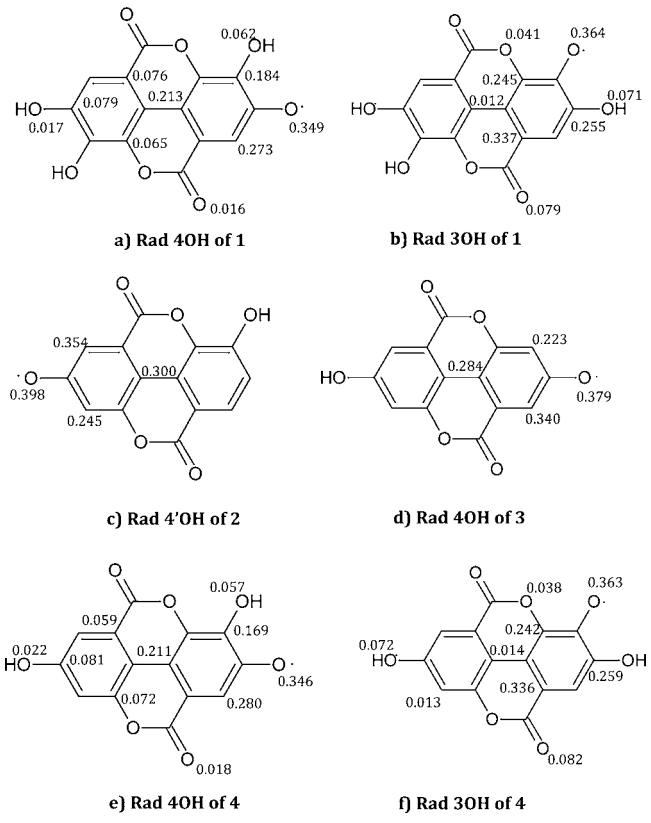

Figure 1. Spin densities of the most stable radical species formed by H removal from the neutral form of each compound.

X-ray diffraction experimental data.[43] The slight differences that sometimes occur fall widely within the experimental error and depend on the different molecular packing of the solid phase, in which experimental measurements were made, with respect to that of the gas phase, typical of theoretical assessments. In the absence of an experimental counterpart, the validity of the used theoretical method in determining geometrical structures allows us to consider reliable also the results obtained for isonasutin (**2**), nasutin A (**3**), and the new derivative (**4**).

Table 3. B3LYP/6-311++G(3df,2p) Relative Enthalpy Energies Calculated for All Compounds and Their Most Stable Radicals Investigated in Both Methanol and Water Environments

compd	BDE (kcal/mol)	IP (kcal/mol)	PDE (kcal/mol)	PA (kcal/mol)	ETE (kcal/mol)
		Methanol			
1	77.3	142.0	252.2	301.5	92.0
2	84.5	146.8	254.6	302.4	98.3
3	82.7	140.7	258.4	303.1	95.3
4	76.9	141.5	252.2	299.4	93.6
		Water			
1	77.3	141.3	252.9	300.5	91.6
2	84.5	146.1	254.3	301.4	98.0
3	82.2	143.9	255.3	302.2	95.0
4	76.9	140.8	251.9	298.5	93.3

Table 4. Energies of HOMO and LUMO for All Compounds Investigated

compd	ε_{HOMO} (eV)	ε_{LUMO} (eV)	$\Delta\varepsilon_{H-L}$ (eV)
1	−0.238	−0.084	0.154
2	−0.245	−0.091	0.154
3	−0.236	−0.095	0.141
4	−0.237	−0.090	0.147

As can be seen in Table 1, from a geometrical point of view, the derivatives do not differ much from ellagic acid, especially in the dilactone functionality. The cases in which the other part of the derivative molecules differs from their precursor are those of isonasutin and nasutin A, because more than one hydroxyl group is removed. Indeed, derivative **4**, which is formed by removing of only one hydroxyl group, has geometric parameters very close to those computed for ellagic acid. The number of possible radical species corresponds to that of hydroxyl groups, except in the case of those compounds (**1** and **3**) for which the number is reduced by half because of the molecular symmetry.

The data in Table 2 indicate that the radicalization of the 4-hydroxyl in ellagic acid (**1**) and its derivative (**4**) leads to a very stable species both in vacuum and in condensed phases, although the energy differences between this and the other possible radicals in both solvents become slightly smaller. In compound **2**, the preferred radicalization site is the 4′-OH, but the 3-OH radical is less stable in both solvents of only 0.2 kcal/mol.

When it is possible to speak of stability order, this reflects the possibility of the particular system to be characterized by a higher contribution of conjugation effects and the presence of an ortho-diphenolic moiety.[26] This can be confirmed by spin density analysis, by which we have obtained the resonance structures of ellagic acid and its most important derivative free radicals (see Figure 1a,b).

The spin density is a reasonably reliable parameter, which provides a better representation of the stability of radical species. According to Parkinson, the more delocalized the spin density in the radical, the more easily is the radical formed.[44]

From the computations concerning the two 3-OH and 4-OH radicals of compounds **1** and **4** (see Figure 1a,b,e,f), it can be observed that in the 4-OH species spin density is delocalized on the whole system, whereas in 3-OH radicals only the ring closer to the radicalization site is involved.

dx.doi.org/10.1021/jf403262k | J. Agric. Food Chem. 2013, 61, 9650−9657

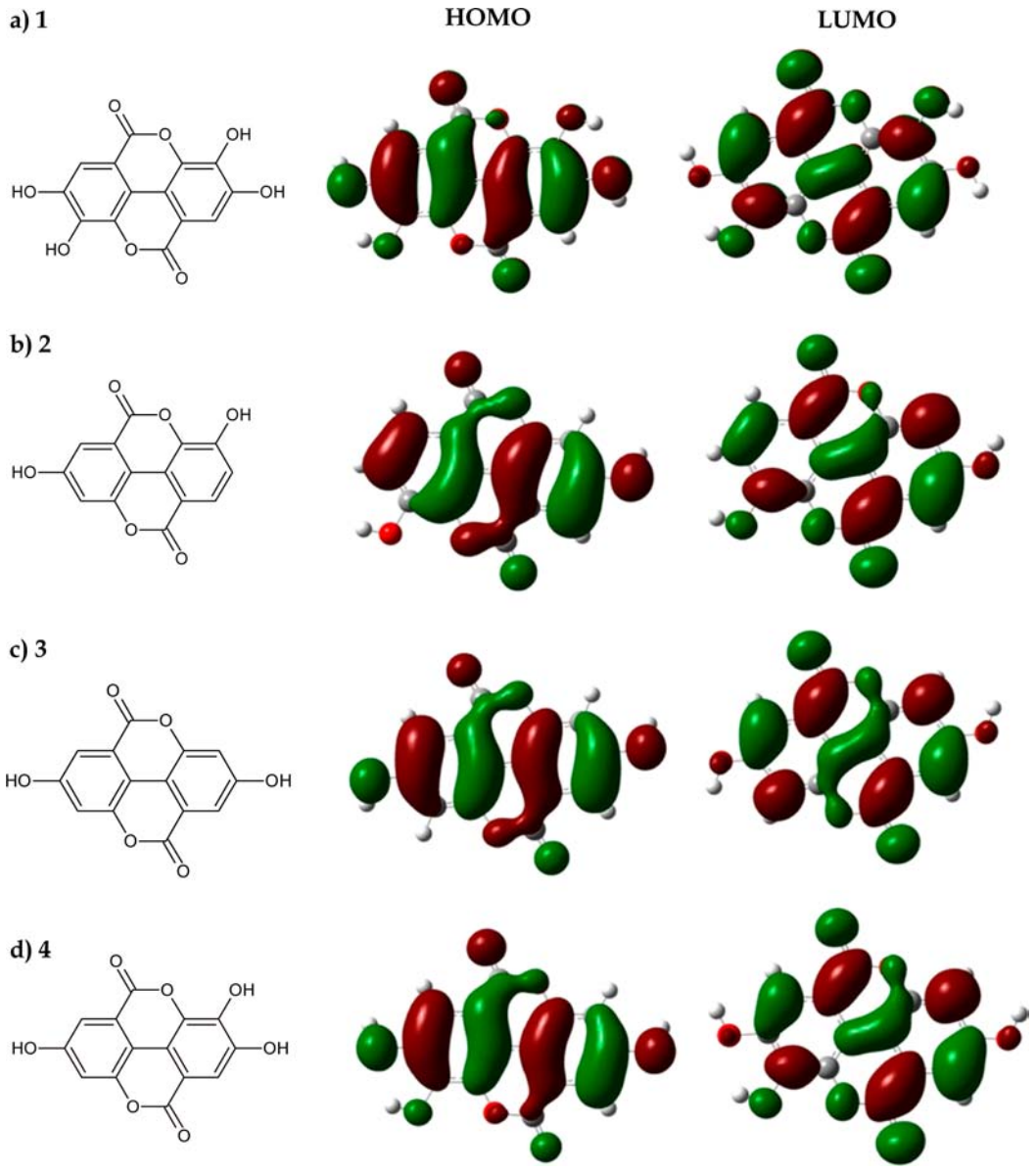

Figure 2. Molecular surface contour plots for the highest occupied and lowest unoccupied molecular orbitals of the investigated compound.

Antioxidant Activity Parameters. In Table 3 we have collected all data concerning the parameters commonly used to define the ability of a compound to act as an antioxidant. Although computations were performed also in the gas phase, the values reported are those obtained in both water and methanol solvents. The latter is the same medium in which the UV−vis spectra were obtained for some of the considered antioxidant molecules.[12]

Results show that the energies put into play in the three considered mechanisms are of very different orders of magnitude.

From a thermodynamic point of view, in both solvents the energy requirement for the HAT mechanism is the lowest for all of the investigated antioxidant molecules. Although for nasutin species **2** and **3** were found values of BDE larger than that computed for ellagic acid, derivative **4** seems to be the best antioxidant because its BDE is found to be 76.9 kcal/mol, which is even smaller than that of **1** (77.3 kcal/mol). The differences in BDE between the latter compounds can be rationalized in terms of differences in the reactivity of the OH sites as we have just explained through the spin density distribution (see Figure 1a,b,e,f).

The formation of radical cations of the studied systems in the first step of the SET-PT mechanism entails an energy expense of 140−147 kcal/mol (see IP values in Table 3) in both solvents. However, data in Table 3 indicate that the next loss of the proton from the $ArOH^{\bullet+}$ is even greater (see PDE values).

In the SPLET mechanism the most crucial step is the formation of phenoxide anion, the proton affinity (PA) of which is very high for all of the investigated compounds. However, also in this case derivative **4** is the most active, because it has the lowest value of proton affinity in both water and methanol solvents. The successive electron transfer from phenoxide anions to free radical occurs quite easily (see ETE values), confirming that the first step is surely that which limits the reaction.

Understanding why a mechanism is favored over another requires the exploration of kinetics, with the evaluation of energetic barriers connecting the various minima on the potential energy surface and energetics aspects of each reaction

Table 5. Main Excitation Energies (ΔE), Oscillator Strengths (f), and MO Contribution at the B3LYP Level of Theory in Solvent[a]

				ΔE		
compd	band	excited state	MO contribution	eV	nm (exptl)	f
1	I	1	H → L (68%)	3.54	351 (365)	0.245
	II	2	H → L+2 (54%)	4.56	272	0.273
		3	H-2 → L+1 (40%)	4.90	253 (253)	0.844
			H-1 → L+2 (45%)			
		4	H-1 → L+2 (48%)	5.05	245	0.601
			H-1 → L (13%)			
2	I	1	H → L (68%)	3.59	346 (331)[b]	0.289
	II	2	H-1 → L+1 (42%)	4.86	255 (259)[b]	0.640
			H-2 → L (18%)			
		3	H-3 → L (61%)	5.12	242	0.202
			H-1 → L+2 (26%)			
		4	H-2 → L+1 (64%)	5.24	237	0.194
		5	H-2 → L+2 (61%)	5.42	229	0.231
3	I	1	H → L (70%)	3.29	377 (373)	0.313
	II	2	H-2 → L (47%)	4.73	262 (*280*)	0.559
			H-1 → L+1 (18%)			
			H-3 → L+1 (18%)			
		3	H-3 → L+1 (59%)	5.36	231 (250)	0.573
			H-1 → L+1 (22%)			
			H-2 → L+2 (19%)			
		4	H-2 → L+5 (63%)	5.64	220	0.342
		5	H-4 → L (69%)	6.01	206	0.246
4	I	1	H → L (69%)	3.40	365	0.267
	II	2	H-3 → L (42%)	4.91	252	0.558
			H-1 → L+2 (26%)			
			H-2 → L+1 (17%)			
		3	H-1 → L+2 (60%)	5.02	247	0.197
			H-3 → L+1 (23%)			
		4	H-2 → L+1 (65%)	5.21	238	0.245
		5	H-1 → L+4 (49%)	6.10	203	0.174

[a]In parentheses are reported the available experimental values.[7] [b]Experimental UV−vis spectrum is for isonasutin A − glucuronide.[7]

step. However, in the case of SET-PT and SPLET, both reaction mechanisms start with a significant energetic disadvantage with respect to the HAT one, although polar solvents such as water or methanol should favor them.

Actually, the charged species formed according to these two mechanisms should have favorable interaction with these kinds of solvent. For this reason we are sure that HAT is the preferred reaction mechanism.

In Table 4, the values of HOMO and LUMO energy are in agreement with the IP trend, confirming that compounds **3** and **4** are the best electron donors, and then they could work hypothetically well following the SET-PT mechanism in which the removal of the hydrogen atom occurs only after that of the electron.

A glance at Figure 2 shows that HOMO and LUMO are delocalized on the whole molecules and are π-like orbitals.

UV Spectra. As reported by González-Barrio et al., the UV spectra of ellagic acid derivatives in methanol exhibit two major absorption peaks in the region 240−400 nm.[12] These two peaks can be referred to as band I (usually 300−380 nm) and band II (usually 240−280 nm) according to the nomenclature generally accepted for flavones.[45] Because the UV experimental spectra of ellagic acid, isonasutin, and nasutin A are available in methanol solvent, we have used this solvent for our TDDFT electronic transition computations. Relative results are reported in Table 5, whereas simulated UV spectra are depicted in Figure 3. For each considered molecule results and discussion will be presented separately, including those of derivative **4** for which no experimental UV spectra are available.

Ellagic Acid. Up to 200 nm region, the experimental UV spectrum of this molecule is characterized by a band of type I with a maximum absorption at 365 nm and a stronger type II band with an absorption maximum at 253 nm. From Table 5 it is clear that the type I band is generated by an electronic transition that falls at 351 nm and involves mainly (68%) HOMO−LUMO (H → L) orbitals. The agreement with the experimental counterpart is very satisfactory, the computed value being blue shifted by only 14 nm. The other band is constituted by three electronic transitions at 272, 253, and 245 nm, which involve the orbitals H → L+2, H-2 → L+1, and H-1 → L+2, respectively, each of which contributes to its electronic transition with percentages of 54, 40, and 48, respectively. The computed transition with the higher value of oscillator strength (0.844) coincides with the experimental maximum (253 nm).

Isonasutin. In this molecule computations indicate a single transition (346 nm) in the type I band region. The measured

dx.doi.org/10.1021/jf403262k | J. Agric. Food Chem. 2013, 61, 9650−9657

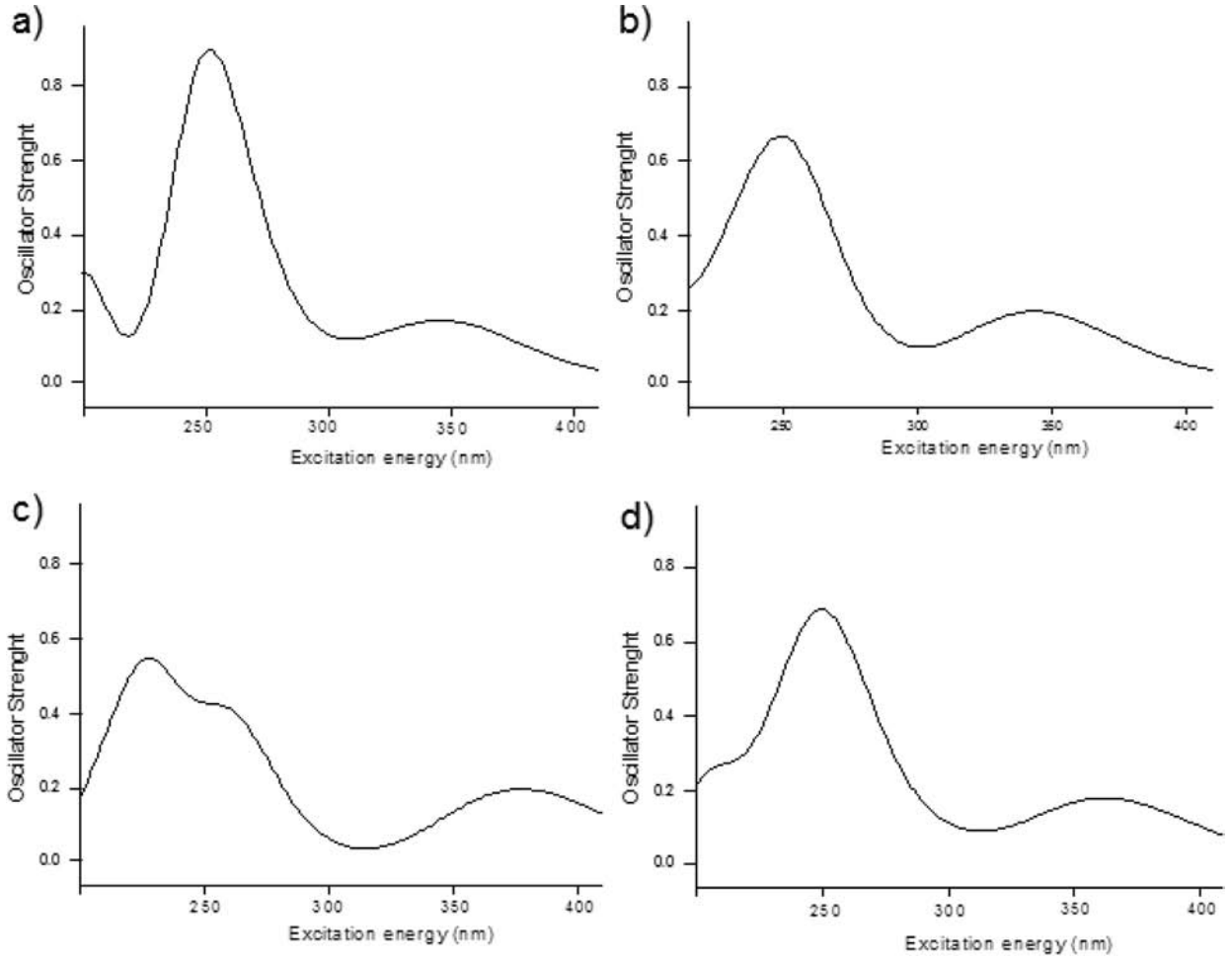

Figure 3. UV spectra computed in methanol of compounds (a) **1**, (b) **2**, (c) **3**, and (d) **4**.

experimental absorption maximum (331 nm), obtained for the isonasutin glucoronide,[12] compares well with our findings. The peak is essentially due to an H → L electronic transition (with a contribution of 68%). A second band involves four transitions at 255, 242, 237, and 229 nm, respectively. The most intense one (255 nm) mainly involves the H-1and L+1 orbitals (42%), whereas the H-2 → L transition contributes with a low percentage (18%). Also in this case a good agreement with experimental data is found (255 versus 259 nm).

Nasutin A. The experimental spectrum of this system is similar to that of both ellagic acid and isonasutin but shows a broader band at high energy. For this system we find an H → L transition (70%) that falls at 377 nm with a deviation of only 4 nm with respect to the experimental data. The type II band includes four transitions (see Table 5), and two of these (at 262 and 231 nm) have comparable intensities (0.559 and 0.573, respectively) as also observed in the experimental shape of the UV spectrum.[12] Both of these transitions are generated by molecular orbitals that lie below the HOMO (see Table 5). Comparison with the experimental results is satisfactory.

Derivative 4. For previous molecules our calculated electronic transitions agree very well with the experimental counterpart, so for this system, for which the experimental UV spectrum is not available, our data can be considered reliable and can serve as a starting point for future and desirable experimental measurements. As expected by some structural consideration, the UV spectrum of this molecule is similar to that of the other considered molecules. At low energy we predict an electronic transition at 365 nm that mainly involves (69%) the H and L orbitals. A more intense band is present at higher energy. As shown in Table 5, four transitions contribute to the shape of this band. The computed transition with the highest value of oscillator strength is located at 252 nm, and it is due to H-3 → L (42%), H-1 → L+2 (26%), and H-2 → L+1 (17%) orbital transitions.

As previously emphasized by experimental studies[12] extended also to the series of urolithins, the comparison between the UV spectra of the studied compounds reveals the important role of the hydroxyl group in position 3 (see Scheme 1). In fact, in going from ellagic acid to nasutin A both hypsochromic and hypochromic shifts are present in band II. On the contrary, the absorption peak in region I is more red-shifted in nasutin A. Similar variations in region II are observed by comparing the spectra of ellagic acid and isonasutin, but in this case also the absorption band in region I is blue shifted.

The origin of the electronic transitions responsible for the UV spectra of the considered molecules is not fully clear, but some conclusions can be drawn. First of all, we observe that the absorption in the band I region is generated in all cases by a $\pi-\pi$ transition as clearly shown by the depicted HOMO and LUMO molecular orbitals (see Figure 2). These orbitals are delocalized on the entire structure, and this means that all of the aromatic rings contribute to the transition. The plot of the other frontier molecular orbitals (see Figures S2 and S3 of

dx.doi.org/10.1021/jf403262k | J. Agric. Food Chem. 2013, 61, 9650−9657

Supporting Information) can give some indications of the origin of the other transition in region II of the spectra. As evidenced in Figures S2 and S3 of the Supporting Information, the other frontier orbitals involved in the transitions (see Table 5) do not have the same extended π nature as in the case of H and L orbitals and in some cases (e.g., H-1 of isonasutin) are localized in specific rings.

In summary, computations performed in gas phase and then in both water and methanol media indicate that the energetics of the various investigated mechanisms is totally different, allowing us to suggest with a good margin of credibility, even in the absence of kinetic data, that the HAT mechanism is preferred in all environments.

The most powerful antioxidant between the examined systems seems to be derivative **4**, which is the only compound not experimentally characterized.

As in previous studies on the same subject, the BDE value, which is the key parameter within the framework of the HAT mechanism, is higher for the systems that have the catechol functionality, which is essential for good stabilization of radical species.

The simulated UV−vis spectra for ellagic acid, nasutin A, and isonasutin are similar to each other and in good agreement with the experimental counterpart. These two pieces of evidence allow us to be very confident also in the reliability of the theoretical spectrum of the new derivative **4**.

■ ASSOCIATED CONTENT

Supporting Information

Fully optimized structures of all the investigated compounds; frontier orbitals involved in the electronic transitions of compounds **1**−**4**, respectively. This material is available free of charge via the Internet at http://pubs.acs.org.

■ AUTHOR INFORMATION

Corresponding Author

*(G.M.) Fax: +39-0984-492044. E-mail: gmazzone@unical.it.

Funding

The University of Calabria, the Food Science and Engineering Interdepartmental Center of University of Calabria, and L.I.P.A.C., Calabrian Laboratory of Food Process Engineering (Regione Calabria APQ − Ricerca Scientifica e Innovazione Tecnologica I atto integrativo, Azione 2 laboratori pubblici di ricerca mission oriented interfiliera, and Azione 3 sostegno alla domanda di innovazione nel settore agroalimentare) are gratefully acknowledged. N.R. thanks UAM for Càtedra Dr. Raùl Remigio Cetina Rosado.

Notes

The authors declare no competing financial interest.

■ REFERENCES

(1) Loarca-Pina, G.; Kuzmicky, P. A.; de Mejia, E. G.; Kadoa, N. Y. Inhibitory effects of ellagic acid on the direct-acting mutagenicity of aflatoxin B1 in the salmonella microsuspension assay. *Mutat. Res.* **1998**, *398*, 183−187.

(2) Castonguay, A.; Boukharta, M.; Teel, R. Biodistribution of, antimutagenic efficacies in *Salmonella typhimurium* of, and inhibition of P450 activities by ellagic acid and one analogue. *Chem. Res. Toxicol.* **1998**, *11*, 1258−1264.

(3) Zafrilla, P.; Ferreres, F.; Tomas-Barberan, F. A. Effect of processing and storage on antioxidant ellagic acid derivatives and flavonoids of raspberry (*Rubus idaeus*) jams. *J. Agric. Food Chem.* **2001**, *49*, 3651−3655.

(4) Ancos, B.; Gonzalez, E. M.; Cano, P. Ellagic acid, vitamin C and total phenolic contents and radical scavenging capacity affected by freezing and frozen storage in raspberry fruit. *J. Agric. Food Chem.* **2000**, *48*, 4565−4570.

(5) Arozarena, I.; Ortiz, J.; Hermosín-Gutiérrez, I.; Urretavizcaya, I.; Salvatierra, S.; Córdova, I.; Marín-Arroyo, M.; Noriega, M. J.; Navarro, M. Color, ellagitannins, anthocyanins and antioxidant activity of Andean blackberry (*Rubus glaucus* Benth.) wines. *J. Agric. Food Chem.* **2012**, *60*, 7463−7473.

(6) Xie, L.; Roto, A. V.; Bolling, B. W. Characterization of ellagitannins, gallotannins and bound proanthocyanidins from California almond (*Prunus dulcis*) varieties. *J. Agric. Food Chem.* **2012**, *60*, 12151−12156.

(7) Escribano-Bailon, M. T.; García-Estévez, I.; Rivas-Gonzalo, J.; Alcalde-Eon, C. Validation of a mass spectrometry method to quantify oak ellagitannins in wine samples. *J. Agric. Food Chem.* **2012**, *60*, 1373−1379.

(8) Vrhovsek, U.; Guella, G.; Gasperotti, M.; Pojer, E.; Zancato, M.; Mattivi, F. Clarifying the identity of the main ellagitannins in the fruit of the strawberry, *Fragaria vesca* and *Fragaria ananassa* Duch. *J. Agric. Food Chem.* **2012**, *60*, 2507−2516.

(9) Teissedre, P.-L.; Michel, J.; Jourdes, M.; Silva, M.; Giordanengo, T.; Mourey, N. Impact of ellagitannins concentration in oak wood on their levels and organoleptic influence in red wine. *J. Agric. Food Chem.* **2011**, *59*, 5677−5683.

(10) Moore, B. P. Coumarin-like substances from Australian termites. *Nature* **1962**, *195*, 1101−1102.

(11) Moore, B. P. The chemistry of the nasutins. *Aust. J. Chem.* **1964**, *17*, 901−907.

(12) González-Barrio, R.; Truchado, P.; Ito, H.; Espín, J. C.; Tomás-Barberán, F. A. UV and MS identification of urolithins and nasutins, the bioavailable metabolites of ellagitannins and ellagic acid in different mammals. *J. Agric. Food Chem.* **2011**, *59*, 1152−1162.

(13) Dorai, T.; Aggarwal, B. B. Role of chemopreventive agents in cancer theraphy. *Cancer Lett.* **2004**, *215*, 129−140.

(14) Seeram, N. P.; Adams, L. S.; Henning, S. M.; Niu, Y.; Zhang, Y.; Nair, M. G.; Heber, D. *In vitro* antiproliferative, apoptotic and antioxidant activities of punicalagin, ellagic acid and a total pomegranate tannin extract are enhanced in combination with other polyphenols as found in pomegranate juice. *J. Nutr. Biochem* **2005**, *16*, 360−367.

(15) Stoner, G. D.; Mukhtar, H. Polyphenols as cancer chemopreventive agents. *J. Cell. Biochem. Suppl.* **1995**, *22*, 169−180.

(16) Festa, F.; Aglitti, T.; Duranti, G.; Ricordy, R.; Perticone, P.; Cozzi, R. Strong antioxidant activity of ellagic acid in mammalian cells *in vitro* revealed by the comet assay. *Anticancer Res.* **2001**, *21*, 3903−3908.

(17) Banzouzi, J.-T.; Prado, R.; Menan, H.; Valenin, A.; Roumestan, C.; Mallie, M.; Pelissier, Y.; Blache, Y. *In vitro* antiplasmodial activity of extracts of *Alchornea cordifolia* and identification of an active constituent: ellagic acid. *J. Ethnopharmacol* **2002**, *81*, 399−401.

(18) Yu, Y.-M.; Chang, W.-C.; Wu, C.-H.; Chiang, S.-Y. Reduction of oxidative stress and apoptosis in hyperlipidemic rabbits by ellagic acid. *J. Nutr. Biochem* **2005**, *16*, 675−681.

(19) Sheu, W.; Kuo, M.-Y.; Ou, H.-C.; Lee, W.-J.; Kuo, W.-W.; Hwang, L.-L.; Song, T.-Y.; Huang, C.-Y.; Chiu, T.-H.; Tsai, K.-L.; Tsai, C.-S. Ellagic acid inhibits oxLDL-induced MMP expression by modulating the PKC-α/ERK/PPAR-γ/NF-κB signaling pathway in endothelial cells. *J. Agric. Food Chem.* **2011**, *59*, 5100−5108.

(20) Martins, D.; Beserra, A.; Calegari, P.; Souza, M.; dos Santos, R.; Lima, J.; Silva, R.; Balogun, S. Gastroprotective and ulcer healing mechanisms of ellagic acid in experimental rats. *J. Agric. Food Chem.* **2011**, *59*, 6957−6965.

(21) Gatto, B.; Furlanetto, V.; Zagotto, G.; Pasquale, R.; Moro, S. Ellagic acid and poly-hydroxylated urolithins are potent catalytic inhibitors of human topoisomerase II: an in vitro study. *J. Agric. Food Chem.* **2012**, *60*, 9162−9170.

(22) Sivachithamparam, N. D.; Kasinathan, N. K.; Subramaniya, B. R.; Natarajan, V. Ellagic acid modulates antioxidant status, ODC

expression and aberrant crypt foci progression in 1,2-dimethylhydrazine instigated colon preneoplastic lesions in rats. *J. Agric. Food Chem.* **2012**, *60*, 3665−3672.
(23) Espín, J. C.; Gonzalez-Sarrias, A.; Miguel, V.; Merino, G.; Lucas, R.; Morales, J.; Tomás-Barberán, F.; Alvarez, A. I. The gut microbiota ellagic acid-derived metabolite urolithin A, and its sulfate conjugate, are substrates for the drug efflux transporter breast cancer resistance protein (ABCG2/BCRP). *J. Agric. Food Chem.* **2013**, *61*, 4352−4359.
(24) Heinonen, I. M.; Kähkönen, M. P.; Kylli, P.; Ollilainen, V.; Salminen, J.-P. Antioxidant activity of isolated ellagitannins from red raspberries and cloudberries. *J. Agric. Food Chem.* **2012**, *60*, 1167−1174.
(25) Craft, B. D.; Kerrihard, A. L.; Amarowicz, R.; Pegg, R. B. Phenol-based antioxidants and the *in vitro* methods used for their assessment. *Compr. Rev. Food Sci. Food Saf.* **2012**, *11*, 148−173.
(26) Leopoldini, M.; Russo, N.; Toscano, M. The molecular basis of working mechanism of natural polyphenolic antioxidants. *Food Chem.* **2011**, *125*, 288−306.
(27) Galano, A. On the direct scavenging activity of melatonin towards hydroxyl and a series of peroxyl radicals. *Phys. Chem. Chem. Phys.* **2011**, *13*, 7147−7157.
(28) Fukui, K. Role of frontier orbitals in chemical reactions. *Science* **1982**, *218*, 747−754.
(29) Frisch, M. J.; Trucks, G. W.; Schlegel, H. B.; Scuseria, G. E.; Robb, M. A.; Cheeseman, J. R.; Montgomery, J. A., Jr.; Vreven, T.; Kudin, K. N.; Burant, J. C.; Millam, J. M.; Iyengar, S. S.; Tomasi, J.; Barone, V.; Mennucci, B.; Cossi, M.; Scalmani, G.; Rega, N.; Petersson, G. A.; Nakatsuji, H.; Hada, M.; Ehara, M.; Toyota, K.; Fukuda, R.; Hasegawa, J.; Ishida, M.; Nakajima, T.; Honda, Y.; Kitao, O.; Nakai, H.; Klene, M.; Li, X.; Knox, J. E.; Hratchian, H. P.; Cross, J. B.; Bakken, V.; Adamo, C.; Jaramillo, J.; Gomperts, R.; Stratmann, R. E.; Yazyev, O.; Austin, A. J.; Cammi, R.; Pomelli, C.; Ochterski, J. W.; Ayala, P. Y.; Morokuma, K.; Voth, G. A.; Salvador, P.; Dannenberg, J. J.; Zakrzewski, V. G.; Dapprich, S.; Daniels, A. D.; Strain, M. C.; Farkas, O.; Malick, D. K.; Rabuck, A. D.; Raghavachari, K.; Foresman, J. B.; Ortiz, J. V.; Cui, Q.; Baboul, A. G.; Clifford, S.; Cioslowski, J.; Stefanov, B. B.; Liu, G.; Liashenko, A.; Piskorz, P.; Komaromi, I.; Martin, R. L.; Fox, D. J.; Keith, T.; Al-Laham, M. A.; Peng, C. Y.; Nanayakkara, A.; Challacombe, M.; Gill, P. M. W.; Johnson, B.; Chen, W.; Wong, M. W.; Gonzalez, C.; Pople, J. A. *Gaussian 03*, revision C.02, Gaussian, Inc.: Wallingford, CT, 2004.
(30) Becke, A. D. Density-functional thermochemistry 3. The role of exact exchange. *J. Chem. Phys.* **1993**, *98*, 5648−5652.
(31) Lee, C.; Yang, W.; Parr, R. G. Development of the Colle−Salvetti correlation−energy formula into a functional of the electron density. *Phys. Rev. B* **1988**, *37*, 785−789.
(32) Cossi, M.; Rega, N.; Scalmani, G.; Barone, V. Energies, structures, and electronic properties of molecules in solution with the C-PCM solvation model. *J. Comput. Chem.* **2003**, *24*, 669−681.
(33) Leopoldini, M.; Marino, T.; Russo, N.; Toscano, M. Antioxidant properties of phenolic compounds: H-atom versus electron transfer mechanism. *J. Phys. Chem. A* **2004**, *108*, 4916−4922.
(34) Leopoldini, M.; Marino, T.; Russo, N.; Toscano, M. Density functional computations of the energetic and spectroscopic parameters of quercetin and its radicals in the gas phase and in solvent. *Theor. Chem. Acc.* **2004**, *111*, 210−216.
(35) Leopoldini, M.; Russo, N.; Toscano, M. Gas and liquid phase acidity of natural antioxidants. *J. Agric. Food Chem.* **2006**, *54*, 3078−3085.
(36) Leopoldini, M.; Chiodo, S. G.; Russo, N.; Toscano, M. Detailed investigation of the OH radical quenching by natural antioxidant caffeic acid studied by quantum mechanical models. *J. Chem. Theory Comput.* **2011**, *7*, 4218−4233.
(37) Mazzone, G.; Malaj, N.; Russo, N.; Toscano, M. Density functional study of the antioxidant activity of some recently synthesized resveratrol analogues. *Food Chem.* **2013**, *141*, 2017−2024.
(38) Iuga, C.; Alvarez-Idaboy, J. R.; Russo, N. Antioxidant activity of *trans*-resveratrol toward hydroxyl and hydroperoxyl radicals: a quantum chemical and computational kinetics study. *J. Org. Chem.* **2012**, *77*, 3868−3877.
(39) Alberto, M. E.; Russo, N.; Grand, A.; Galano, A. A physicochemical examination of the free radical scavenging activity of Trolox: mechanism, kinetics and influence of the environment. *Phys. Chem. Chem. Phys.* **2013**, *15*, 4642−4650.
(40) Bartmess, J. Thermodynamics of the electron and the proton. *Phys. Chem.* **1994**, *98*, 6420−6424.
(41) Klein, E.; Lukeš, V. DFT/B3LYP study of the substituent effect on the reaction enthalpies of the individual steps of single electron transfer-proton transfer and sequential proton loss electron transfer mechanisms of phenols antioxidant action. *J. Phys. Chem. A* **2006**, *110*, 12312−12320.
(42) Casida, M. E. *Recent Advances in Density Functional Methods*, Part I; Chong, D. P., Ed.; World Scientific: Singapore, 1995.
(43) Rossi, M.; Erlebacher, J.; Zacharias, D. E.; Carrel, H. L.; Iannucci, B. The crystal and molecular structure of ellagic acid dihydrate − a dietary anticancer agent. *Carcinogenesis* **1991**, *12*, 2227−2232.
(44) Parkinson, C. J.; Mayer, P. M.; Radom, L. An assessment of theoretical procedures for the calculation of reliable radical stabilization energies. *J. Chem. Soc., Perkin Trans. 2* **1999**, 2305−2313.
(45) Mabry, T. J.; Markham, K. R.; Thomas, M. B. *The Systematic Identification of Flavonoids*; Springer Verlag: Berlin, Germany, 1970.